

Fermi resonance in Ne, Ar and Kr-matrix infrared spectra of 5-bromouracil

A.Yu. Ivanov, Yu.V. Rubin, S.A. Egupov, L.F. Belous, and V.A. Karachevtsev

*B. Verkin Institute for Low Temperature Physics and Engineering of the National Academy of Sciences of Ukraine
47 Lenin Ave., Kharkov 61103, Ukraine
E-mail: ivanov@ilt.kharkov.ua*

Received December 21, 2012, revised February 13, 2013

Low-temperature matrix isolation Fourier-transform infrared spectroscopy and quantum-chemical calculations with DFT/B3LYP and MP2 methods were used for investigation of isolated 5-bromouracil (BrU) molecules. Only one tautomeric form of BrU was dominated in the low-temperature Ne, Ar, and Kr matrices. It was revealed that population of minor hydroxy-tautomers did not exceed 0.2%. Appearance of additional absorption bands in the region of stretching vibrations ν_{CO} (about 1710 cm^{-1}) as well as of deformation ones ($1297, 1093, 901\text{ cm}^{-1}$) was explained by Fermi resonance. In Ne matrices the peak intensities of absorption bands assigned to the out-of-plane vibrations of the ring and exocyclic atoms were decreased sharply. For the first time, least square method with the using of polynomial was proposed for the corrective scaling of calculated frequencies of vibrations. It is shown that the correction of calculated frequencies with the polynomial of degree two permits to decrease the root-mean-square discrepancy between the calculated and experimental ones to $4\text{--}5\text{ cm}^{-1}$ in the region of $1500\text{--}500\text{ cm}^{-1}$. The same polynomial may be applied for the correction of spectra of molecules with a similar structure.

PACS: **33.15.-e** Properties of molecules;
33.20.-t Molecular spectra;
33.20.Ea Fourier transform spectra;
82.30.Qt Isomerization and rearrangement.

Keywords: FTIR spectroscopy, matrix isolation, DFT method, Fermi resonance.

1. Introduction

Modern science shows constant interest in studies of biological molecules under conditions free of strong intermolecular interactions [1,2]. The low-temperature spectral methods are the basis of this scientific direction [1–5]. Low-temperatures permit to freeze separate isomers of biological molecules and their complexes in the inert surrounding and to model biological processes in the space [6]. Besides, absent of molecule rotation in the inert medium permits essential improve of the resolution of vibrational spectra. Owing to this, the low-temperature matrix isolation infrared spectroscopy revealed self-descriptiveness technique during studies on tautomerism of deoxyribonucleic acid (DNA) bases and of their biologically active derivatives [7]. Such biologically active molecules as halogen-substituted DNA bases and nucleosides have a vital part in the various biological processes [8]. For example, 5-haloderivatives of uracil are able to replace thymine in

DNA [8,9], have increased mutagenic activity [8,10] and increase DNA sensitivity to ionizing radiation [11]. Some works were devoted to studies of vibrational spectra of 5-bromouracil (BrU) molecules isolated in Ar matrices [12–14]. On the basis of these spectra, conclusions have been made on BrU flat structure [12] and on Fermi resonance in the region of ν_{CO} stretching vibrations [13,14]. As well, the conclusion on the predominance of the tautomeric structure of BrU₀ was drawn (Fig. 1).

However, in spite of the predominance BrU₀ tautomer, the number of absorption bands in the experimental vibrational spectra of BrU exceeds noticeably theoretically possible $3N-6$ fundamental vibrations. Also, quantitative data on BrU tautomeric equilibrium and on low-intensity spectral bands in the deformation range of $1500\text{--}500\text{ cm}^{-1}$ were absent. Meanwhile, analysis of the uracil spectra reveals Fermi resonance in this spectral region ($1550\text{--}500\text{ cm}^{-1}$) too [15]. Besides, spectra of BrU were obtained only for Ar matrices, and this is able to complicate their analysis

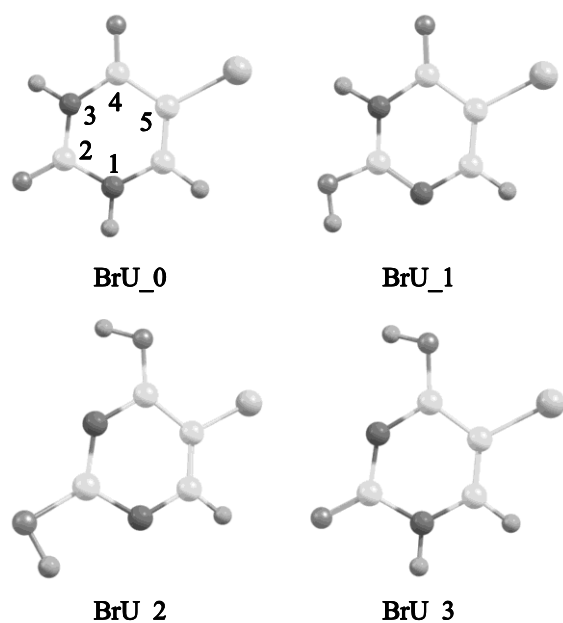


Fig. 1. Molecular structure and atom numbering of the main BrU tautomers.

owing to the matrix effect on the vibrational spectrum. The matrix induces frequency shifts of spectral bands. As a result, the multiplex structure of contour of absorption band may occur. The appearance of multiplexes is often associated with stable conformations of the matrix sites [16,17] as well with the interaction with the matrix through libration of the impurity molecules [18]. It is evident that the more lattice parameters of inert matrices will differ the more noticeable differences in spectra of molecules isolated in matrices will be. Therefore, in our work, the vibrational spectra of isolated BrU molecules were obtained not only in the matrices with relatively close lattice parameters (Ar, Kr) but in Ne matrices also. To calculate vibrational spectra by the DFT/B3LYP method, in addition to correlation consistent basis sets, 6-311++G(df, pd) one was used, revealed the best results in some works [19,20]. For the first time, to scale the calculated frequencies, we employed the least square method with the corrective multiplier as the polynomial. On the basis of the vibrational spectrum of isolated molecules, the proposed scheme of investigation interprets structure of isolated BrU molecules more reliably.

2. Experimental and computer modeling methods

Main details of the low-temperature experiment were presented in works [21–24]. In the present investigation Fourier-transform infrared (FTIR) spectra were measured in the range of $3800\text{--}500\text{ cm}^{-1}$, with apodized resolution being 0.25 cm^{-1} . Matrix deposition onto cryogenic mirrors was controlled with the low-temperature quartz crystal microbalance (QCM) [25]. The molecular flow intensity and the concentration of impurity molecules were measured by QCM (the matrix-to-sample ratio = M/S). The in-

tensity of the molecular flow of commercial BrU samples (Sigma) was about $(50\text{--}60)\cdot 10^{-9}\text{ g}/(\text{s}\cdot\text{cm}^2)$ at evaporation temperatures $440\text{--}460\text{ K}$. In this temperature range thermal destruction of BrU molecules was not observed. The purity of inert gases (Ne, Ar, and Kr) exceeds 99.99%. The temperatures of cryogenic mirrors were 5 K for Ne matrices and 12 K for Ar and Kr matrices.

Quantum-chemical calculations were performed with Gaussian 09 [26] and Firefly QC (version 7.1.G) [27] program packages. Firefly QC package is partially used the GAMESS (US) program code [28]. Structures of the BrU were optimized at the density functional theory DFT/B3LYP [29] and Möller–Plesset perturbation theory (MP2) level of theory. As well, CCSD(T) and complete basis set (CBS) methods [30] and correlation consistent basis sets aug-cc-pVDZ, aug-cc-pVTZ [31] were used. DFT/B3LYP method with basis sets aug-cc-pVDZ and aug-cc-VTZ and 6-311++G(df,pd) was applied to calculate vibrational spectra.

Standard capabilities of Firefly program were used for the estimation of Gibbs free energies (ΔG) of BrU tautomers. At analysis of spectra the representing normal modes through internal coordinates by INTC program were used [32,33]. Calculated spectra were synthesized by SYNSPEC program [34] for the visual comparison of experiment and calculations.

3. Results and discussion

3.1. Scaling of DFT/B3LYP frequencies with the least square method

A frequently used density functional theory (DFT) method of calculation was applied to assign the absorption bands of the experimental vibrational spectra. In comparison with MP2 method, DFT one not only reduces the computation time but partly compensates the manifestation of the anharmonicity of real vibrations [35]. Actually for comparison with the experiment, multiplication of calculated frequencies by the corrective multiplier λ (the “scaling factor”) is necessary. Besides, as indicated above, additional frequency shifts are caused by the matrix. It is known that, in comparison with the gas phase, for frequencies higher than 1000 cm^{-1} matrix shifts as a rule are negative and can be positive for frequencies lower than 1000 cm^{-1} [16]. In our experiments the shifts frequency of the spectral bands of BrU isolated in Ar and Kr matrices with regard to the spectrum in Ne matrix were determined (Fig. 2). For the stretching vibrations in the region $3500\text{--}1600\text{ cm}^{-1}$ these shifts are negative and depend monotonically on the frequency (Fig. 2). In the deformation region of $1500\text{--}500\text{ cm}^{-1}$ the shifts may be different signs and may depend on frequency non-monotonous (Fig. 2).

For scaling of calculated frequencies the constant value of λ is usually used, fitted for one or two frequencies of the

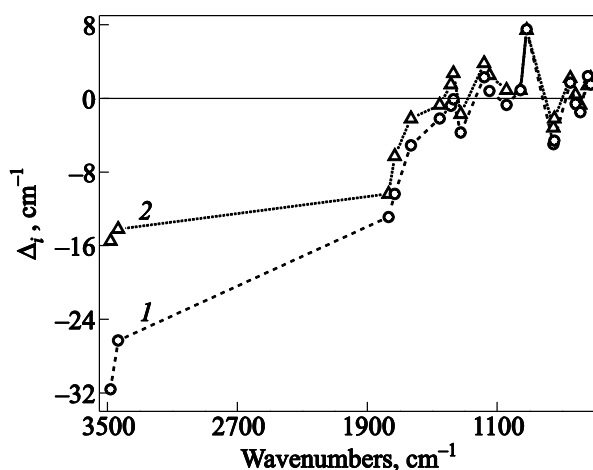


Fig. 2. Frequency shifts (Δ_i , cm^{-1}) of absorption bands of the experimental BrU spectra in Kr (1) and Ar (2) matrices in relation to Ne matrix. The dotted lines between Δ_i are drawn for clear illustration.

spectral range. To optimize λ in the whole range, it was proposed to use the least square method [36] in which the minimum of error function S is the optimum criterion [37]:

$$S = \sum_i^N \omega_i - \lambda v_i^2 \rightarrow \min, \quad (1)$$

where ω_i is the experimental frequency, v_i is the calculated frequency.

Minimum of the expression (1) is found from condition $\partial S / \partial \lambda = 0$:

$$\lambda = \frac{\sum_i^N \omega_i v_i}{\sum_i^N v_i^2}. \quad (2)$$

It is seen from the representation of frequency shifts (Fig. 2) that correction by the constant λ is satisfactory only in the narrow frequency range. Frequency scaling for the deformation range must be performed with the nonmonotonous function. Therefore, the computer program was elaborated for the correction of frequencies with the polynomial of degree M : $X_0 + X_1 f + \dots + X_M f^M$. Then, the error function S may be presented as

$$S = \sum_i^N \left[\omega_i - \left(\sum_{k=0}^M X_k f_i^k \right) v_i \right]^2 \rightarrow \min. \quad (3)$$

From conditions of minimum of the expression (3) the system of linear equations is obtained:

$$\frac{\partial S}{\partial X_{j=0 \dots M}} = 2 \sum_i^N \left[\omega_i - \sum_{k=0}^M X_k f_i^k v_i \right] (-f_i^j v_i) = 0. \quad (4)$$

Gaussian method [38] was used for the numerical solution of the system of linear algebraic equations (Eq. (4)). Next, the computer program determined the mean deviation $\Delta_m = (\sum \Delta_i) / N$, maximum deviation $\Delta_{\max} = \max |\Delta_i - \Delta_m|$ and root-mean-square deviation $\delta_{rms} = [(\sum (\Delta_i - \Delta_m)^2) / N]^{1/2}$ of the corrected raw of calculated frequencies from the experimental ones of the vibrational spectrum.

The vibrational spectra for the dominating structure of BrU were calculated by DFT/B3LYP method. Statistical results of the frequency correction with the fixed multiplier as well as with polynomials of degree one and two in the range of 1550–500 cm^{-1} are presented in Table 1. It follows from these results that linear regression ($M = 1$) is practically no better than scaling with the fixed λ ($M = 0$). However, regression with the polynomial of degree two which is a nonmonotonous function profits markedly for the all parameters (Table 1). Relative to the linear regression, advantage of nonmonotonous one for aug-cc-pVTZ basis is higher than that for aug-cc-pVDZ basis. However, both the correlation bases rank below to 6–311++G(df,pd) not only in the nonmonotonous regression but in the least values of Δ_{\max} , δ_{rms} and K (Table 1). This verified the conclusion of the previous works on efficiency of the DFT/B3LYP/6–311++G(df,pd) method for calculations of vibrational spectra [19,20]. Besides, 6–311++G(df,pd) basis requires smaller computational cost than aug-cc-pVTZ one. The tapping of the more time consuming the DFT/B3LYP/aug-cc-pVTZ/anharmonic method only affects the results of the frequency correction (Table 1). The best approximation of calculation to experiment is obtained for BrU in Ne matrices. The values Δ_{\max} and δ_{rms} for Ar and Kr matrices coincide practically (Table 1). In spite of the nonmonotonous frequency shift of spectral bands in Ar and Kr matrices (Fig. 2), the increasing of δ_{rms} does not exceed 20% in comparison with Ne matrix (Table 1).

To check polynomials obtained for BrU on other molecules, the spectral data for glycine [39] and uracil [21] were used. Linear regression demonstrates close results for both molecules (Table 1). The polynomial of degree two increases sharply value of Δ_{\max} and δ_{rms} for glycine. However, for uracil, magnitudes of the values of Δ_{\max} and δ_{rms} decrease (Table 1). Evidently, the increase of the polynomial degree restricts the range of its use by molecules of the similar structure.

The scaling of calculated spectra allows us to perform the reliable assignment of the absorption bands in FTIR spectra. The absorption bands of the stretching and bending vibrations of the ring and exocyclic groups are arranged in the range of 1500–1000 cm^{-1} . A comparison of the calculated and experimental spectrum in this region shows a good agreement of the frequencies of spectral bands (Fig. 3). Only two weak absorption bands at 1297 and 1093 cm^{-1} require the further discussion. In the range of 1000–500 cm^{-1} half of absorption bands belong out-of-plane bending vibrations of the ring and exocyclic groups.

Table 1. Statistical parameters of discrepancies between experimental frequencies of BrU in Ne, Ar, Kr matrices and frequencies calculated by DFT/B3LYP method with different basis sets and polynomial corrections

Basis sets	Degree of polynomial	Δ_m, cm^{-1}			$\delta_{rms}, \text{cm}^{-1}$			$\Delta_{max}, \text{cm}^{-1}$			K
		Ne	Ar	Kr	Ne	Ar	Kr	Ne	Ar	Kr	
aug-cc-pVDZ	$M=1$	-0.3	-0.3	-0.3	11.2	11.6	11.4	25.8	24.8	24.5	9
aug-cc-pVDZ	$M=2$	0.1	0.2	0.1	9.6	9.6	9.4	22.8	21.3	21.3	7
aug-cc-pVTZ	$M=0$	-0.7	0.3	-0.6	7.6	8.4	8.3	14.9	13.8	13.5	8
aug-cc-pVTZ	$M=1$	-0.3	-0.3	-0.3	7.6	8.3	8.3	13.8	12.8	12.9	8
aug-cc-pVTZ	$M=2$	0.1	0.1	0.1	5.6	6.1	6.1	11.2	13.0	13.7	6
aug-cc-pVTZ ^a	$M=1$	-0.5	-0.6	-0.6	10.5	11.2	11.2	21.4	22.2	21.9	10
aug-cc-pVTZ ^a	$M=2$	0.0	0.0	0.0	7.2	8.0	8.0	13.5	16.1	16.9	8
6-311++G(df,pd)	$M=0$	0.3	-0.6	0.4	7.1	8.1	8.2	12.3	17.8	19.0	10
6-311++G(df,pd)	$M=1$	-0.4	-0.4	-0.4	6.7	7.8	7.8	10.7	16.8	18.0	9
6-311++G(df,pd)	$M=2$	0.0	0.0	0.0	4.3 ^d	5.1	5.2	9.9	12.0	12.8	4
aug-cc-pVDZ ^b	$M=1$		-1			8.2			17.3		
aug-cc-pVDZ ^b	$M=2$		-1.4			12.0			25.4		
aug-cc-pVDZ ^c	$M=1$		-1.4			10.4			23.2		
aug-cc-pVDZ ^c	$M=2$		-0.7			8.7			21.0		

Notes: ^a anharmonic calculation; ^b correction of glycine frequencies [39] by BrU polynomial for Ar matrices; ^c correction of uracil frequencies [21] by BrU polynomial for Ar matrices; ^d for Ne matrices the polynomial may be presented as $0.9267 + v(1.38 \cdot 10^{-4}) - v^2(6.86 \cdot 10^{-8})$; K is the number of bands with discrepancy greater than 6 cm^{-1} .

Here comparison demonstrates a good agreement between the calculated and experimental bands too, except the weak band at 901 cm^{-1} (Fig. 4).

3.2. Occupation of BrU tautomers in the low-temperature matrices

The calculations show that the hydroxy tautomers have considerably greater energy than the major diketoform. Varying methods of calculation and basis sets does not lead to the significant changes ($< 2 \text{ kJ/mol}$) of relative energies (Table 2). Also, consideration of Gibbs free energy

does not change the relative stability of the BrU tautomers. Based on these data, using the standard formula, we can calculate the population of tautomer j at temperature T [40]:

$$O_j(T) = \frac{\exp(-\Delta G_j(T)/RT)}{\sum_{i=0}^n \exp(-\Delta G_i(T)/RT)} 100\% . \quad (5)$$

The temperature plots of population minor of the BrU tautomers were obtained by using Eq. (5). According to these plots the population of the BrU₁-BrU₂ tautomers

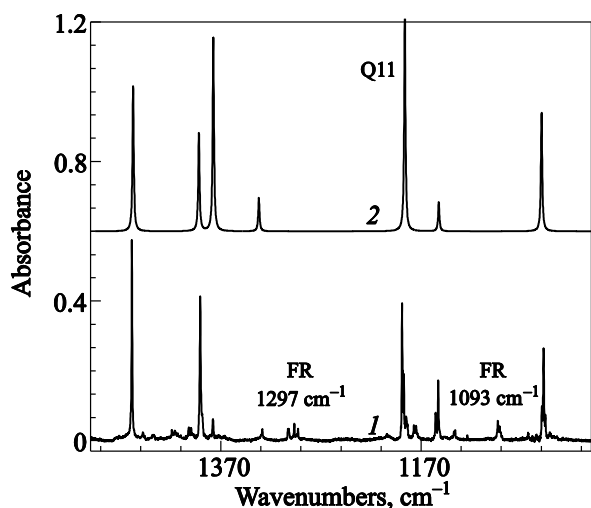


Fig. 3. Vibrational spectra in the region of stretching vibrations of pyrimidine ring and BrU deformation vibrations ($1500\text{--}1000 \text{ cm}^{-1}$): Ar matrix ($T = 11 \text{ K}$, $M/S = 800:1$) (1); calculation by DFT/B3LYP/ 6-311++G(df,pd) method with frequency correction of the polynomial of degree two (2). FR is combination bands enhanced by Fermi resonance.

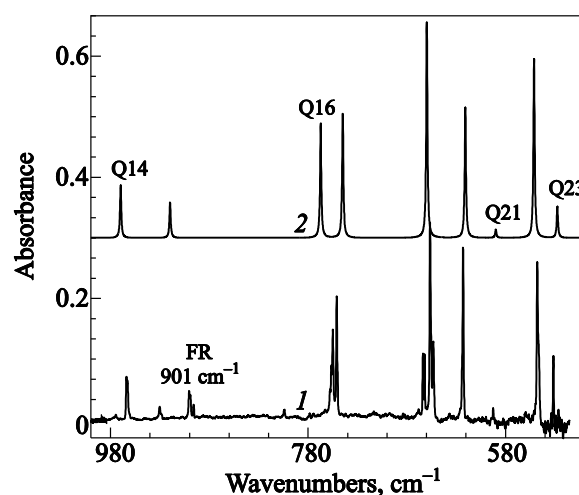


Fig. 4. Vibrational spectra in the BrU deformation region ($1000\text{--}500 \text{ cm}^{-1}$): Ar matrix ($T = 11 \text{ K}$, $M/S = 800:1$) (1); calculation by DFT/B3LYP/ 6-311++G(df,pd) method with frequency correction of the polynomial of degree two (2). FR is combination bands enhanced by Fermi resonance.

should not exceed 0.02% in the temperature range of this work (440–460 K) (Fig. 5). The data of calculation are in a good agreement with experiment. The search of characteristic absorption bands was performed in the range of ν_{CO} stretching vibrations, which are the most intense vibrations of the BrU tautomers. Comparison of experimental and calculated data demonstrates absence of characteristic bands of ν_{CO} vibrations for the BrU_1 and BrU_2 tautomers (accuracy of estimation at 0.2% population).

Table 2. Full (E , a.u) and relative energies (ΔE , ΔG , kJ/mol) of main BrU tautomers calculated by the different *ab initio* methods

Tautomer	Method	ΔE , MP2/aug-cc-pVTZ	ΔE , MP2/CBS	ΔE , CCSD(T)/ MP2/aug-cc-pVDZ	ΔG (460 K)*, kJ/mol
BrU_0	(E, -2986.2276)	(E, -2986.5215)	(E, -2985.8023)		
		0	0	0	0
BrU_1		36.2	35.5	35.4	35.6
BrU_2		36.7	35.0	37.9	37.3
BrU_3		47.5	46.8	47.2	46.9

Notes: *averaging of ΔE over the first three columns of table was used at calculations of ΔG .

3.3. Fermi resonance in the ν_{CO} range and the range of deformation vibrations

The overwhelming dominance of the BrU_0 tautomer over other tautomer structures permits to suggest that additional spectral bands, not assigned to calculated ones, have a resonance nature. Splitting of bands due to Fermi resonance can be observed in the vibrational spectra of the pyrimidine bases in the low-temperature matrices [19,21,41,42]. By analogy with these studies, the BrU_0 absorption bands about 1710 cm^{-1} (Figs. 6(a), (c)) may belong to combination bands enhanced by Fermi resonance. For the rigorous proof of this fact, it is necessary to consider as intensities

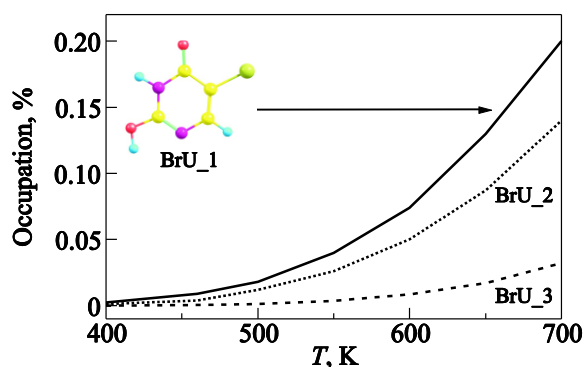


Fig. 5. Temperature evaporation dependent of the population of minor BrU tautomers.

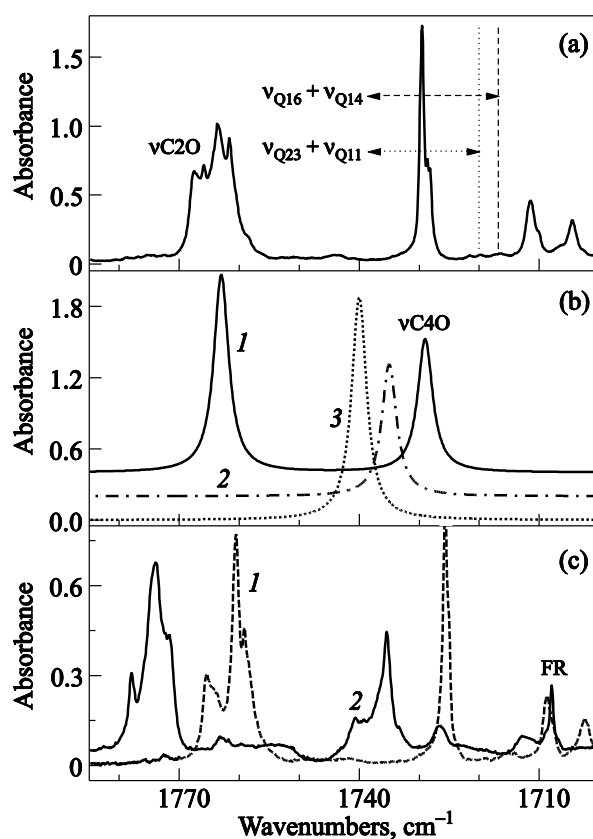


Fig. 6. Vibrational spectra in the ν_{CO} stretching region of BrU: (a) Ar matrix ($T = 11 \text{ K}$, $M/S = 800:1$); vertical dotted line indicate the possible combination bands; (b) calculation by DFT/B3LYP/ 6–311++G(df,pd) method for BrU_0 (1); BrU_1 (2), and BrU_3 (3); (c) Kr matrix ($T = 11 \text{ K}$, $M/S = 800:1$) (1); Ne matrix ($T = 5 \text{ K}$, $M/S = 700:1$) (2).

of vibrations involved in the Fermi resonance are changed. Under resonance, redistribution of intensities of the fundamental I_f and combination I_c vibrations is taking place [43]:

$$I_c / I_f = (\Delta - \Delta_0) / (\Delta + \Delta_0), \quad (6)$$

where Δ_0 is the initial difference of frequencies between the fundamental and combination vibration, and Δ is the total splitting of bands. Since $\Delta = \Delta_{\text{res}} + \Delta_0$, Eq. (6) can be transformed to

$$I_c / I_f = \Delta_{\text{res}} / (\Delta_{\text{res}} + 2\Delta_0), \quad (7)$$

where Δ_{res} is the resonance splitting of bands.

It follows from Eq. (7) that ratio of intensities can be changed if you change the Δ_0 , for example, using matrix shifts of vibration frequencies. It depends on the nature of interacting vibrations. Fundamental and combination vibrations that have the same properties of symmetry are involved in Fermi resonance [43]. For example, the ν_{CO} fundamental vibrations and combination vibrations formed by stretching and flat deformation vibrations of pyrimidine

ring or side groups. The Fig. 2 presents that frequency of ν_{CO} increases in Ne matrix in comparison with Ar or Kr matrices. In comparison with the ν_{CO} , the absolute value of frequency shifts of the deformation vibrations is less and can have a different sign. Consequently, if the initial frequency of combination vibration in Ar matrix is less than frequency of fundamental vibration ν_{CO} , then under going to Ne matrix the Δ_0 value may increase. Then, according to Eq. (7), the intensity of the combination band should decrease. It is precisely these changes in the intensity of the absorption bands about 1710 cm^{-1} were observed in the BrU experimental spectra BrU (Fig. 6, Table 3). Integral intensities of combination bands in Ar and Kr matrices are the same, but they sharply decrease in the Ne matrix (Table 3).

Table 3. Frequencies and intensities of absorption bands measured in the ν_{CO} stretching region in Ne, Ar and Kr matrices

Vibration	Ar matrix		Kr matrix		Ne matrix	
	ν^a, cm^{-1}	I^b	ν, cm^{-1}	I^b	ν, cm^{-1}	I^b
ν_{C2O}	1763.4	1	1760.1	1	1774.1	1
ν_{C4O}	1729.5	0.4	1725.7	0.4	1735.3	0.49
Combination band	1711.4	0.28	1708.7	0.29	1707.9	0.12

Notes: ^aFrequency of the most intensive band in multiplet (Fig. 6(a), 6(c)); ^bintegral intensity is normalized to ν_{C2O} intensity.

This is strong evidence that absorption bands about 1710 cm^{-1} are among the combination vibrations. These vibrations may be formed by the normal mode Q11 (Fig. 3), Q14, Q16, and Q23 (Fig. 4). Hitherto, to study the Fermi resonance of ν_{CO} vibrations for uracil [21] and isocytosine [20] we used the same method of matrix shifts. The weak bands $1297, 1093\text{ cm}^{-1}$ (Fig. 3) and 901 cm^{-1} (Fig. 4) may also be assigned to the Fermi resonance-enhanced combination bands. Previously, Fermi resonance has been demonstrated in this area for uracil [19] and isocytosine [20].

Besides absorption bands, which do not correspond to the calculated spectra we can see close satellites of fundamental vibrations in the experimental spectra (Figs. 3, 4, 6, 7). The interaction with the matrix through librations of the impurity molecule may be a probable hypothesis of complex structure of multiplets. It was shown previously, that due to librations one of bending vibrations of methane molecules in Xe matrix undergoes a dramatic broadening of absorption band with a corresponding decreasing of peak intensity. As well, a decreasing of peak intensities of some bands in the deformation region was found in the FTIR spectra of BrU in Ne matrices. The most characteristic changes are related to the out-of-plane bending vibrations of NH groups (Fig. 7). The band of N3H group bending vibration not only dramatically reduces the peak intensity in the Ne ma-

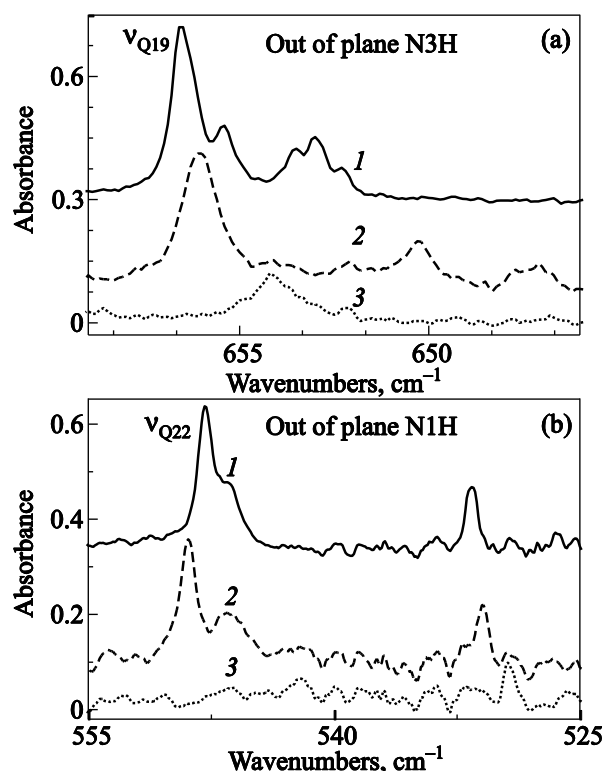


Fig. 7. The variation frequency and intensity of BrU deformation vibration of NH groups in the Ar (1), Kr (2) and Ne (3) matrices: (a) out-of-plane vibration of N3H; (b) out-of-plane vibration of N1H.

trix, but is shifted to lower frequencies region (Fig. 7(a)). The band of bending vibration of N1H group almost disappears from the spectrum in Ne matrix, and as well, its frequency is also reduced. Reduction of peak intensity in Ne matrix was observed for all out-of plane vibrations of BrU.

4. Conclusions

It was established that only one tautomeric form of 5-bromouracil dominated in the low-temperature matrices, as the population of the minor tautomers does not exceed 0.2%.

The least squares method was used for the scaling of calculated frequencies by using polynomial. It is shown that the use of the polynomial to adjust the frequency obtained by the DFT/B3LYP method reduces the mean square discrepancy between theory and experiment to $4\text{--}5\text{ cm}^{-1}$. The common polynomial may be used to scale frequencies of vibrations of molecules with similar structure. The use of the 6-311++G(df,pd) basis set and Ar matrices may be an optimal choice for the investigations of vibrational spectra of biological molecules.

Owing to Fermi resonance in the BrU spectra, some additional absorption bands appear in the ν_{CO} stretching vibrations region ($\sim 1710\text{ cm}^{-1}$), and region of bending vibrations ($1297, 1093, 901\text{ cm}^{-1}$). It was found that in the

Ne matrix, the peak intensities of the absorption bands of out-of-plane bending vibrations of the ring and exocyclic atoms of BrU decreases sharply.

Acknowledgment

The present work was carried out due to the financial support (grant No. 0110U007895) of the National Academy of Sciences of Ukraine. The authors thank S.G. Stepanian for helpful discussions and R.I. Zubatyuk for his help in organization and carrying out of calculations. Quantum-chemical calculations were performed using computational cluster of B. Verkin Institute for Low Temperature Physics and Engineering of National Academy of Science of Ukraine and computational facilities of joint computational cluster of SSI "Institute for Single Crystals" and Institute for Scintillation Materials of National Academy of Science of Ukraine incorporated into Ukrainian National Grid.

1. E.G. Robertson and J.P. Simons, *Phys. Chem. Chem. Phys.* **3**, 1 (2001).
2. R. Weinkauff, J.-P. Schermann, M.S. de Vries, and K. Kleiner-manns, *Eur. Phys. J.* **D20**, 309 (2002).
3. M. Hartmann, R.E. Miller, J.P. Toennis, and A. Vilesov, *Phys. Rev. Lett.* **75**, 1566 (1995).
4. F. Huisken, O. Werhahn, A.Yu. Ivanov, and S.A. Krasnokutski, *J. Chem. Phys.* **111**, 2978 (1999).
5. M.Y. Choi and R.E. Miller, *J. Phys. Chem. A* **111**, 2475 (2007).
6. Z. Peeters, O. Botta, S.B. Charnley, R. Ruiterkamp, and P. Ehrenfreund, *Astrophys. J.* **593**, 129 (2003).
7. Yu.P. Blagoi, G.G. Sheina, A.Yu. Ivanov, E.D. Radchenko, M.V. Kosevich, V.S. Shelkovsky, O.A. Boryak, and Yu.V. Rubin, *Fiz. Nizk. Temp.* **25**, 1003 (1999) [*Low Temp. Phys.* **25**, 747 (1999)].
8. W. Saenger, *Principles of Nucleic Acids Structure*, Springer-Verlag, New York (1984).
9. S. Zamenhof, B. Reiner, R. De Giovanni, and K. Rich, *J. Bio. Chem.* **219**, 165 (1956).
10. O.O. Brovarets and D.M. Hovorun, *Ukr. Bio. Acta* **2**, 19 (2009) (in Ukrainian).
11. H. Abdoul-Carime, M.A. Huels, E. Illenberger, and L. Sanche, *J. Am. Chem. Soc.* **123**, 5354 (2001).
12. S.G. Stepanian, E.D. Radchenko, G.G. Sheina, and Yu.P. Blagoi, *Biofizika* **34**, 753 (1989).
13. M. Graindourze, T. Grootaers, J. Smets, Th. Zeegers-Huyskens, and G. Maes, *J. Mol. Struct.* **237**, 389 (1990).
14. J.Cz. Dobrowolski, J.E. Rode, Robert Kołos, M.H. Jamróz, K. Bajdor, and A.P. Mazurek, *J. Phys. Chem. A* **109**, 2167 (2005).
15. C. Puzzarini, M. Biczysko, and V. Barone, *J. Chem. Theory Comput.* **7**, 3702 (2011).
16. S. Cradock and A.J. Hincliffe, *Matrix Isolation*, Cambridge University Press, New York (1975).
17. A.M. Plokhotnichenko, E.D. Radchenko, Yu.P. Blagoi, and V.A. Karachevtsev, *Fiz. Nizk. Temp.* **27**, 901 (2001) [*Low Temp. Phys.* **27**, 666 (2001)].
18. S.T. Collins, P.A. Casey, and G.C. Pimentel, *J. Chem. Phys.* **88**, 7307 (1988).
19. W. Zierkiewicz, L. Komorowski, D. Michalska, J. Cerny, and P. Hobza, *J. Phys. Chem. B* **112**, 16374 (2008).
20. A.Yu. Ivanov, S.G. Stepanian, and L. Adamowicz, *J. Mol. Struct.* **1025**, 92 (2012).
21. A.Yu. Ivanov, A.M. Plokhotnichenko, E.D. Radchenko, G.G. Sheina, and Yu.P. Blagoi, *J. Mol. Struct.* **372**, 91 (1995).
22. A.Yu. Ivanov, G.G. Sheina, and Yu.P. Blagoi, *Spectrochim. Acta A* **55**, 219 (1999).
23. A.Yu. Ivanov, S.A. Krasnokutski, G. Sheina, and Yu.P. Blagoi, *Spectrochim. Acta A* **59**, 1959 (2003).
24. A.Yu. Ivanov and V.A. Karachevtsev, *Fiz. Nizk. Temp.* **33**, 1772 (2007) [*Low Temp. Phys.* **33**, 590 (2007)].
25. A.Yu. Ivanov and A.M. Plokhotnichenko, *Instr. Experim. Techn.* **52**, 308 (2009).
26. *Gaussian 09, Revision A.02*, M.J. Frisch, G.W. Trucks, H.B. Schlegel, G.E. Scuseria, M.A. Robb, J.R. Cheeseman, G. Scalmani, V. Barone, B. Mennucci, G.A. Petersson, H. Nakatsuji, M. Caricato, X. Li, H.P. Hratchian, A.F. Izmaylov, J. Bloino, G. Zheng, J.L. Sonnenberg, M. Hada, M. Ehara, K. Toyota, R. Fukuda, J. Hasegawa, M. Ishida, T. Nakajima, Y. Honda, O. Kitao, H. Nakai, T. Vreven, J.A. Montgomery, Jr., J.E. Peralta, F. Ogliaro, M. Bearpark, J.J. Heyd, E. Brothers, K.N. Kudin, V.N. Staroverov, R. Kobayashi, J. Normand, K. Raghavachari, A. Rendell, J.C. Burant, S.S. Iyengar, J. Tomasi, M. Cossi, N. Rega, J.M. Millam, M. Klene, J.E. Knox, J.B. Cross, V. Bakken, C. Adamo, J. Jaramillo, R. Gomperts, R.E. Stratmann, O. Yazyev, A.J. Austin, R. Cammi, C. Pomelli, J.W. Ochterski, R.L. Martin, K. Morokuma, V.G. Zakrzewski, G.A. Voth, P. Salvador, J.J. Dannenberg, S. Dapprich, A.D. Daniels, Ö. Farkas, J.B. Foresman, J.V. Ortiz, J. Cioslowski, and D.J. Fox, Gaussian, Inc., Wallingford CT (2009).
27. A.A. Granovsky, *Firefly, version 7.1G*, <http://classic-chem.msu.su/gran/firefly/index.html> (2009).
28. M.W. Schmidt, K.K. Baldridge, J.A. Boatz, S.T. Elbert, M.S. Gordon, J.H. Jensen, S. Koseki, N. Matsunaga, K.A. Nguyen, S. Su, T.L. Windus, M. Dupuis, and J.A. Montgomery, *J. Comput. Chem.* **14**, 1347 (1993).
29. A.D. Becke, *Phys. Rev. A* **38**, 3098 (1988).
30. D.G. Truhlar, *Chem. Phys. Lett.* **294**, 45 (1998).
31. T.H. Dunning, Jr., *J. Chem. Phys.* **90**, 1007 (1989).
32. P. Pulay, G. Fogarasi, F. Pang, and J.E. Boggs, *J. Am. Chem. Soc.* **101**, 2550 (1979).
33. G. Fogarasi, X. Zhou, P.W. Taylor, and P. Pulay, *J. Am. Chem. Soc.* **114**, 8191 (1992).
34. K. Irikura, *Program SYNSPEC*, National Institute of Standards and Technology, Gaithersburg, MD20899, USA (1995).
35. G.M. Chaban and R.B. Gerber, *Theor. Chem. Acc.* **120**, 273 (2008).
36. A.P. Scott and L. Radom, *J. Phys. Chem.* **100**, 16502 (1996).

37. G.R. Cooper and C.D. McGillem, *Probabilistic Methods of Signal and System Analysis*, CBS College Publishing (1986).
38. I.I. Molchanov, *Machine Methods of Solution of Applied Tasks. Algebra, Approximation of Functions*, Naykova Dymka, Kuiv (1987) (in Russian).
39. S.G. Stepanian, I.D. Reva, E.D. Radchenko, and L. Adamowicz, *J. Phys. Chem. A* **102**, 4623 (1998).
40. J.H. Jensen and M.S. Gordon *J. Am. Chem. Soc.* **113**, 7917 (1991).
41. K. Szczepaniak, M.M. Szczesniak, and W.B. Person, *J. Phys. Chem. A* **104**, 3852 (2000).
42. B. Morzyk-Ociepa, M.J. Nowak, and D. Michalska, *Spectrochim. Acta A* **60**, 2113 (2004).
43. M.P. Lisitsa and A.M. Yaremko, *Fermi Resonance*, Naykova Dymka, Kuiv (1984) (in Russian).